Front. Electr. Electron. Eng. China 2007, 2(4): 404–409
DOI 10.1007/s11460-007-0075-y

RESEARCH ARTICLE

YAN Songhua, WU Shicai, WEN Biyang

Low velocity target detection based on time-frequency image for high frequency ground wave radar

© Higher Education Press and Springer-Verlag 2007

Abstract The Doppler spectral broadening resulted from non-stationary movement of target and radio-frequency interference will decrease the veracity of target detection by high frequency ground wave (HFGW) radar. By displaying the change of signal energy on two dimensional time-frequency images based on time-frequency analysis, a new mathematical morphology method to distinguish target from nonlinear time-frequency curves is presented. The analyzed results from the measured data verify that with this new method the target can be detected correctly from wide Doppler spectrum.

Keywords time-frequency analysis, mathematical morphology, HFGW, target detection

1 Introduction

High frequency (HF) radar system has been widely developed to detect and track targets in wide area of surveillance across long ranges, such as Raytheon's long-range HF radar located at Cape Race [1], HF Surface Over-the-Horizon Radar set up by Harbin Institute of Technology [2], and Wuhan University's ocean state measuring and analyzing radar (OSMAR). For these radars, constant false alarm rate (CFAR) processors based on the Fourier transform are typical target detection methods. However, CFAR detection algorithms often produce many false targets when applied to HF radar. There are two reasons for the invalidation. The long coherent integration time (CIT) is the first disadvantage. When using the Fourier transform properly, it is assumed that the frequency contents of the signal must be time-invariant. However, most of the target for HFGW radar moves in a randomly determined direction or velocity during the long CIT, and then Doppler frequency shifts are time-varying. Thus the Doppler spectrum is broadened by accelerating or decelerating longitudinal velocity. The other reason is that HFGW radar systems must deal with the problem of user congestion in the high frequency band (3–30 MHz). Radio frequency interferences (RFIs), such as short duration communication signals among ships, may cause false peak in the Doppler spectrum, or the target signals will be submerged in clutter signals, especially under low signal-noise-ratio (SNR) environment.

As is reported, there exist some RFI suppression methods that possess good performance, such as detecting instantaneous interference in range-time sequence by wavelet transform [3], interference nulling technology using horizontal dipole antennas [4,5], and adaptive beam forming algorithm [6], etc. Nevertheless, all those cannot overcome the problem of spectrum broadening.

Time-frequency representations provide direct and efficient ways to analyze the time-frequency structure of signals; therefore, they are widely used for non-stationary signal analysis, for example, detecting airplanes' moving at high speed [7]. Chirp signal is one of the typical non-stationary signals to model airplane and Hough transform is a classical method for long chirp detection.

In HF radar, however, due to the targets' non-stationary movements and various interference conditions, a normal chirp mode is not valid. Therefore, it is necessary to find a more effective way for target detection.

In this paper, via substituting time-frequency transform for the Fourier transform in the conventional Doppler domain, a time-frequency image is constructed. This image provides different energy congregating areas which symbolize different signals. Then a method based on mathematical morphology instead of straight-line detection is presented. This method distinguishes the target from the interferences by its time duration, so the method can overcome the problem of spectrum broadening.

Translated from *Chinese Journal of Radio Science*, 2006, 21(3): 391–396 [译自: 电波科学学报]

YAN Songhua (✉), WU Shicai, WEN Biyang
School of Electronic Information, Wuhan University, Wuhan 430072, China
E-mail: ysh567@sohu.com

2 Fast Fourier transform (FFT) and Doppler spectrum

2.1 Doppler spectrum of HF radar echo signal

The HFGW radar transmits N linear frequency modulated (FM) pulses in a CIT, and demodulates the echo signal by converting it with an FM Local oscillator signal. M samples are taken from a pulse and after the first FFT, the range profile is got. Then N samples are taken from the same range cell and after the second FFT, Doppler spectrum that corresponds to the velocity profile is obtained. The following equations can show the process.

When a target located on mth range cell, the nth sample is [8]

$$S_{nm} = K\exp\left(\mathrm{i}2\pi f_c \frac{2V}{c} nT\right) = K\exp\left(\mathrm{i}2\pi f_c \frac{2V}{c} t_n\right) \tag{1}$$

where K is amplitude, V is radial velocity, T is period, c is the speed of light and f_c is the operating frequency.

After the second FFT, the spectrum is

$$S_m(f) = KNT \frac{\sin\left[2\pi\left(f - \frac{2V}{c} f_c\right) NT/2\right]}{\left[2\pi\left(f - \frac{2V}{c} f_c\right) NT/2\right]} \tag{2}$$

The peak of the spectrum $2Vf_c/c$ corresponds to the target.

Figure 1 demonstrates Doppler spectra of a real echo signal, where sea clutter components are two large spectral spikes around zero-Doppler that are known as Bragg lines while the target is a spike at around −0.6 Hz. Bragg lines provide the sea state information. However, it is noisy for target detection. Thus, to overcome that problem, locating Bragg lines and excluding it from the detection range are utilized [9]. For simplicity, the ensuing discussion is based on the assumption that the area encompassing Bragg lines have been detected and excluded from the detection area in the frequency domain.

2.2 Doppler spectrum broadening

The simple processing by doubling FFTs encounters plenty of limitations. First RFIs may show as peaks on the Doppler spectrum. Second, in CIT both the direction and velocity change of the maneuvering target may lead to the broadening of Doppler spectrum.

A normal Doppler shift of a target can be expressed as

$$f_\mathrm{d} = \frac{2V}{c} f_c \cos\theta \tag{3}$$

where V symbolizes velocity, θ is the angle between the target direction and the normal line of the antenna array.

While the target changes its direction from θ_1 to θ_2, the Doppler shift is

$$f_\mathrm{d} = \frac{2(V + at)}{c} f_c \cos\theta_2 \tag{4}$$

where a is target acceleration.

The Doppler spectra of radar echo signals in different conditions are shown in Fig. 2.

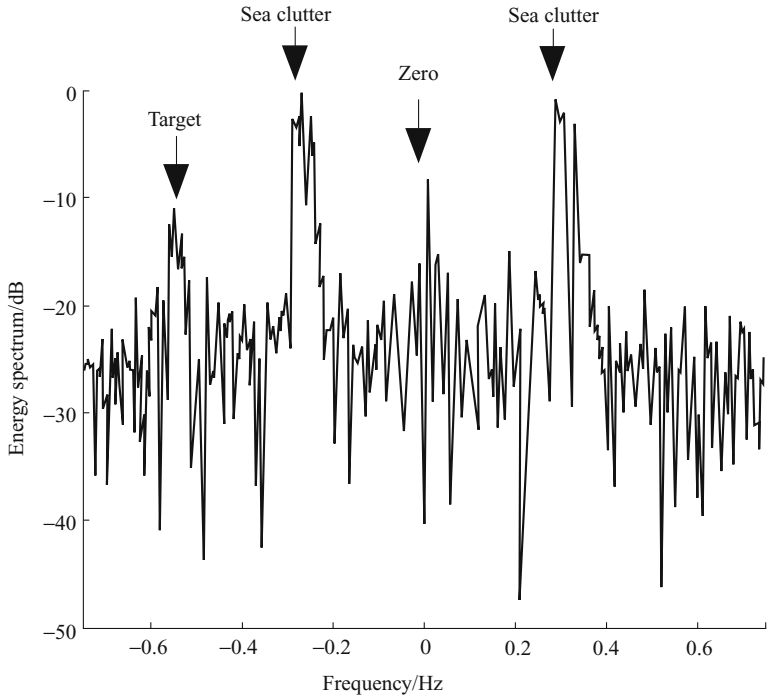

Fig. 1 Doppler spectrum of HF radar echo signal

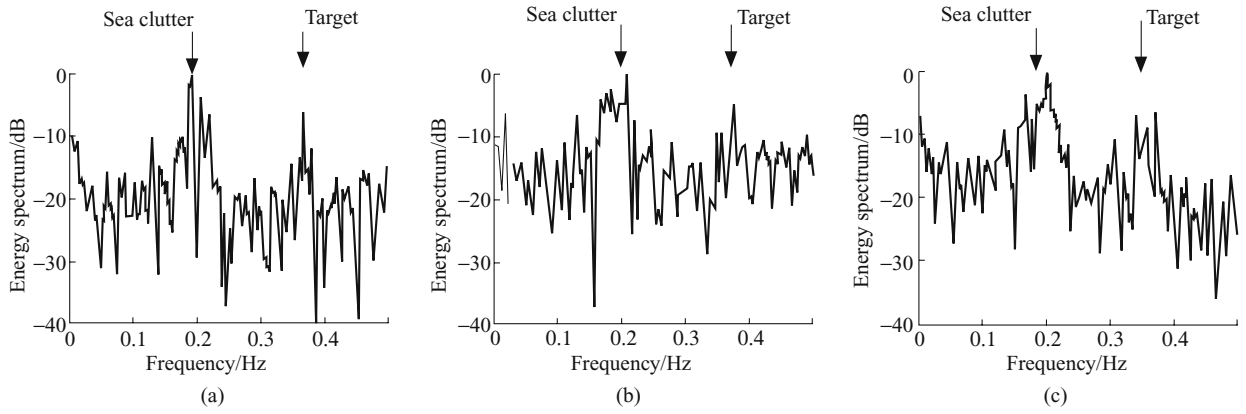

Fig. 2 Doppler spectra of HF radar echo signals in different conditions
(a) Normal Doppler spectrum without spectrum broadening; (b) broadened frequency spectrum by noise; (c) broadened frequency spectrum by target motion

Figure 2(a) shows the Doppler spectrum without frequency broadening, where signal noise ratio (SNR) is about 10 dB and the target can be seen in the spectrum as a spike at 0.38 Hz corresponding to the target radial velocity of 10.4 m/s. In Fig. 2(b) and (c) Doppler spectra spread widely from approximately 0.33 to 0.42 Hz. It is undeterminable that whether the target accelerates, decelerates, or whether there exist RFIs near the Doppler frequency. It can be known from later analysis that Doppler spectrum broadening in Fig. 2(b) is mostly resulted from RFIs, while in Fig. 2(c) spectrum broadening is for the most part caused by the target motion. However, due to the similarity of target echo broadening and background RFIs, the target in the Doppler spectrum cannot be distinguished. Some methods, such as auto focusing, are utilized for solving Doppler smearing problem. However, because many methods are Fourier-based approaches, they cannot reveal the time feature of the signal and consequently cannot acquire satisfactory results.

3 Short-time-Fourier-transform (STFT) processing

3.1 FFT and STFT

Time-frequency analysis, such as linear time-frequency transform and double linear time-frequency distribution, can describe intensity distribution of signals both in time and frequency domain. In order to avoid the cross items, STFT instead of FFT is utilized to handle the original data and obtain time-frequency two-dimensional images.

If $x(t)$ is the signal to be analyzed, define STFT as

$$F_x^h(t,f)=\int_{-\infty}^{+\infty} x(\tau)h^*(\tau-t)\mathrm{e}^{-\mathrm{j}2\pi\tau}\mathrm{d}\tau \tag{5}$$

In Eq. (5), $h(\tau)$ is the analysis window centering on $\tau=0$. $h^*(\tau)$ denotes complex conjugation and t represents the center time of the analysis interval on $x(\tau)$, the localized STFT spectrum is simply the magnitude of the STFT.

$$S_x^h(t,f)=\left|F_x^h(t,f)\right|^2 \tag{6}$$

Because STFT spectrum is a local spectrum of the signal [10] around the analysis time as shown in Fig. 3, it can reveal the frequency changes in a time-frequency image. Because the tradeoff in time-frequency concentration (temporal resolution versus frequency resolution) depends on the selection of the analysis window shape and duration, the parameters were chosen to provide the best resolution of the target.

Then FFT is substituted by STFT to process the original data.

It can be concluded from Eq. (1) that the signal in every range cell is analytic. Subsequently Eq. (1) can be rewritten as below

$$S_{nm}=K\cos\left(2\pi f_c\frac{2V}{c}nT\right)+\mathrm{i}K\sin\left(2\pi f_c\frac{2V}{c}nT\right) \tag{7}$$

Note that the corresponding spectra of both real and image part of S_{nm} can represent the structure of spectrum. Therefore, STFT first is adopted to deal with the image part of original data, then two-dimensional pictures are acquired by squaring, which show energy changes of signals in time and frequency domain.

3.2 Time-frequency images of echoes

A target tracking experiment was carried out in the East Sea of China in 2004 with OSMAR system located on Zhujiajian Island in Zhejiang Province. The major parameters of the radar are listed in Table 1. Figure 2 in Section 2.2 demonstrates the processing result of the original data in this experiment by FFT.

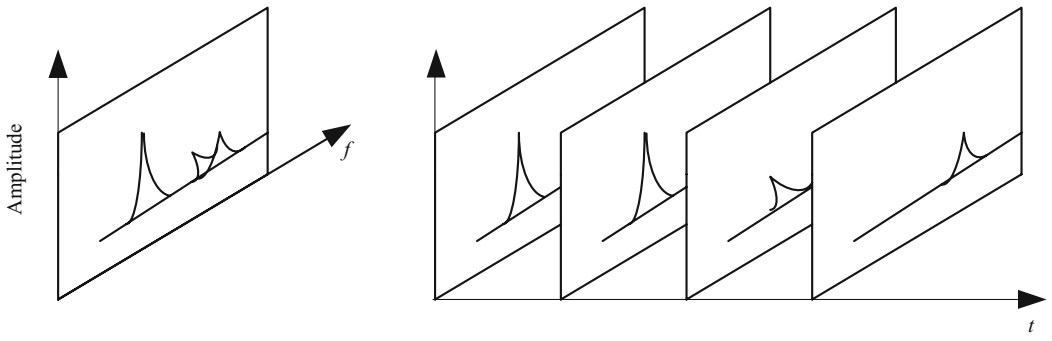

Fig. 3 Spectra by FFT and STFT

Table 1 Major parameters of OSMAR system

Parameter	Value	Parameter	Value
Radar waveform	FMICW	Range resolution	2.5 km
Operating frequency	7 MHz	Sweep frequency band	60 kHz
Samples per block	256	Waveform repetition frequency	1.53 Hz
Coherent integration time	167 s	Sweep period	0.652 8 s
Range	200 km	Max velocity of target	15 m/s

The calculation of STFT spectrum of original data in Fig. 2 turns out high-resolution time-frequency images as shown in Fig. 4, where the grey level is used to indicate the magnitude and the frequency is normalized by sample frequency.

Figure 4(a) shows a straight line at the invariable normalized frequency 0.38 Hz, which obviously stands for a target of constant radial velocity of 10.4 m/s. In Fig. 4(b) there are five curves between normalized frequency 0.35 and 0.5 Hz, and it is obvious that the long stretching line symbolizes the target, while those short duration lines denote RFIs during the CIT. Figure 4(c) shows a snake-like curve around 0.37 Hz that clearly reveals the changes of the Doppler frequency due to the change of target velocity or direction.

4 Target detection with mathematical morphology method

Target detection from the gray image is a problem of pattern recognition. A time frequency image can be viewed as a bivariate distribution of signal energy per time/frequency. Because the target is shown as a snake-like curve, the typical method for straight-line detection is no longer appropriate. In Fig. 4 both the target signal and RFIs are shown as areas with energy conglomeration in the time-frequency image, and the main difference between the two items is the length of duration. The target signal almost exists in the whole CIT. While RFIs only exist for a short time. This character is represented in the image by different length of the high gray level area.

Mathematical morphology is a tool for extracting image components by providing a quantitative description of geometrical structures of objects, such as boundaries, skeletons and convex hulls [11]. To extract the time duration, a set of mathematical morphological operations is employed to segment the image and identify the target by its length. Taking Fig. 4 for example, the operating steps are as follows.

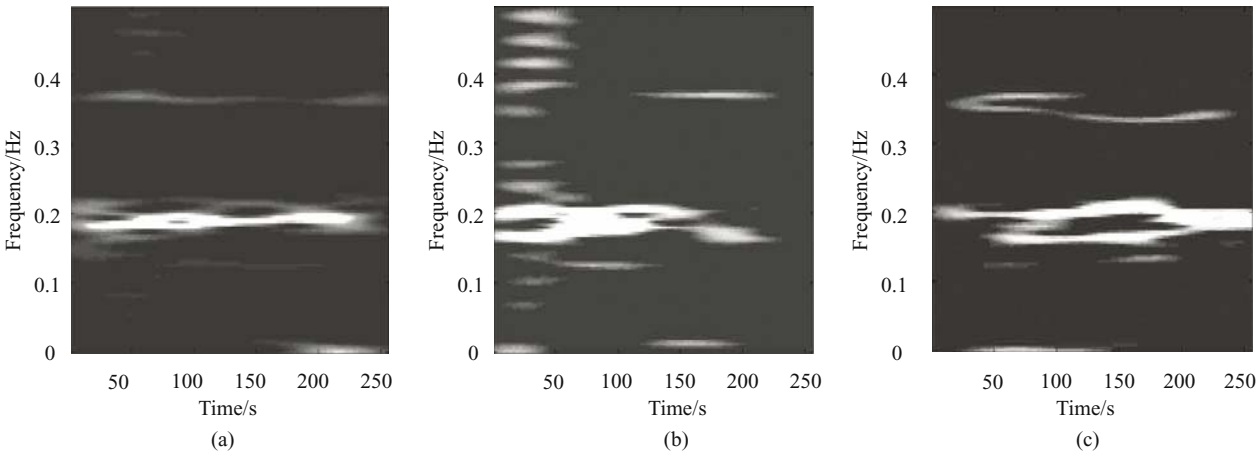

Fig. 4 Time-frequency images of radar echoes
(a) Constant velocity target signal; (b) target signal and RFIs; (c) various velocity target signal

1) Pre-process the image: find the area containing Bragg lines and exclude them from the detection area.

2) Determine the gray-level threshold and transform the gray-level image into a binary one. Gray-level threshold is the simplest segmentation process; here double peak method [12] is utilized to choose the threshold.

3) Carry out morphological opening (dilation after erosion) of the binary image with proper structuring element $\boldsymbol{B}$. Morphological opening can eliminate clumps smaller than the structuring element, such as short time RFIs, while the global shape of objectives is not distorted. Here the structuring element $\boldsymbol{B}$ is a typical diamondoid element [13]

$$\boldsymbol{B} = \begin{bmatrix} 0 & 1 & 0 \\ 1 & 1 & 1 \\ 0 & 1 & 0 \end{bmatrix}$$

4) Implement morphological skeleton algorithm: skeletons can convert the object to an archetypical stick figure, preserve the connectivity and simplify the shape.

5) Mark each skeleton first, and then calculate the length of it. When the length of a skeleton exceeds a certain threshold, the target detection is declared.

After mathematical morphology operating on Fig. 4, the skeletons of different objects are got in Fig. 5. Here sea clutter areas are not eliminated from the image in order to compare with Fig. 4. Figure 5(a) shows a long line representing a target that is undergoing uniform motion. In Fig. 5(b) there exist some lines, but only the line whose length exceeds the length threshold is judged to be target while others are identified as RFIs. In Fig. 5(c) the line changes in a snake-like manner that reveals the details of the instantaneous frequency and it is identified as target on account of its length.

By continuously observing and analyzing the acquired data in the East Sea of China, it can be concluded that RFIs caused by communication between ships generally last no more than 2 min. Thus 2 min, as a time threshold, is short enough for HF radar to divide target from RFIs.

Because skeletons can display details of instantaneous frequency changes and mathematical morphology can tell the differences in length between target and RFIs, this detecting method will avoid false decision that may occur in CFAR based on FFT.

5 Target and sea clutter

The sea-clutter region is a blind spot of high frequency radar detection [14]. Thus the effect of mathematical morphology method mentioned above gets worse when Doppler spectrum of target signal falls into the area of sea clutter. Figure 6(a) displays the situation when target signal passes through the sea-clutter region. In the figure, one slope line with highlight represents the objective, and the other approximately horizontal lines denote sea clutter. Figure 6(b) is obtained using mathematical morphology method. This picture demonstrates that the two objects are differentiated from skeleton drawings when there is some offset between Doppler frequency and sea-clutter frequency. However, when the two become closer, skeletons of the two will combine together, which can not be distinguished. At this moment, sea clutter should initially be suppressed or other characters of target should be made use of, such as the difference in the slope, instantaneous frequency changes and so on [15].

6 Conclusion

In this paper, a novel method is proposed for target detection and applied to HF radar system. Because both instantaneous interference and non-stationary movement of target may produce Doppler spectrum broadening, joint time-frequency representation is adopted because it provides excellent ways to analyze non-stationary signals, and its improved capacity to display frequency changes with time is an advancement of Fourier analysis. With mathematical morphology, the target is distinguished from the short time RFIs by its long skeleton

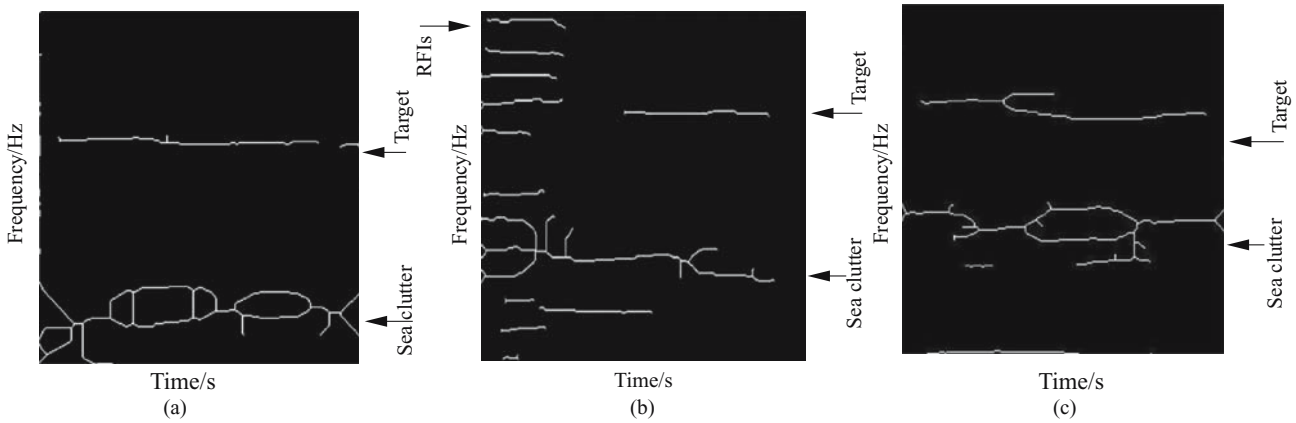

Fig. 5 Skeletons of target signal and RFIs
(a) Constant velocity target signal; (b) target signal and RFIs; (c) various velocity target signal

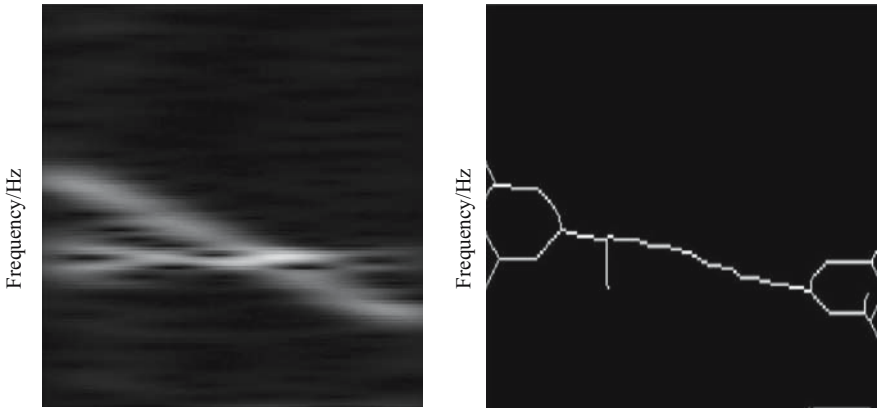

Fig. 6 Target "passes through" sea clutters
(a) Time frequency image; (b) morphology skeleton

length. Experimental results show that the target can be efficiently and reliably detected using this method.

In the practical processing, the window function and gray level threshold have strong impact on the detection result. Therefore, how to choose them entails more research in the future.

Acknowledgements This work was supported by the Hi-Tech Research and Development Program of China (No. 2001AA631050).

References

1. Blake T M. Ship detection and tracking using high frequency surface wave radar. In: Proceedings of the 7th IEEE International Conference on HF Radio Systems and Techniques. Nottingham, UK: IEE, 1997, 291–295
2. Wang Wei, Peng Yingning, Quan Taifan, et al. HF OTHR target detection and estimation subsystem. IEEE AES Systems Magazine, 1999, 14(2): 39–45
3. Huang Liang, Wen Biyang, Deng Wei. Suppressing instantaneous interference of high frequency ground wave radar. Chinese Journal of Radio Science, 2004, 19(2): 166–170 (in Chinese)
4. Yang Jun, Wen Biyang, Wu Shicai, et al. Study of interference nulling using horizontal dipole antennas. Chinese Journal of Radio Science, 2004, 19(2): 176–181 (in Chinese)
5. Zhang Guoyi, Liu Yongtan. Study of the polarization filtering technique of HF ground wave radar. Systems Engineering and Electronics, 2000, 22(3): 55–57 (in Chinese)
6. Su Hongtao, Bao Zheng, Zhang Shouhong. Adaptive HF-communication interference mitigation in HF-GWR. Chinese Journal of Radio Science, 2003, 18(3): 270–274 (in Chinese)
7. Hu Juan, Zhang Jun. Time-frequency distribution and multi-target resolution of radar signal. Radar & ECM, 2003, 3(3): 26–29 (in Chinese)
8. Wu Shicai, Yang Zijie, Wen Biyang, et al. Waveform analysis for HF ground wave radar. Journal of Wuhan University (Natural Science Edition), 2001, 47(5): 519–527 (in Chinese)
9. Zhang Yi, Ke Hengyu, Wen Biyang, et al. A new method to estimate signal number by echos phase. Journal of Wuhan University (Natural Science Edition), 2003, 49(1): 137–140 (in Chinese)
10. Zhang Xianda, Bao Zheng. Analysis and Process of the Non-Static Random Signal. Beijing: National Defense Industry Press, 1998 (in Chinese)
11. Gong Wei, Shi Qingyun, Cheng Minde. Mathematical Morphology in Digital Space—Theory and Application. Beijing: Science Press, 1997 (in Chinese)
12. Han Siqi, Wang Lei. A survey of thresholding methods for image segmentation. Systems and Electronics, 2002, 24(6): 91–94 (in Chinese)
13. Sonka M, Hlavac V, Boyle R. Image Processing, Analysis and Machine Vision. USA: Thomson Asia Pteled, 2002
14. Fan Junmei, Jiao Peinan, Xiao Jingming. The sea clutter effect on the low Doppler targets detection by HF radar. Chinese Journal of Radio Science, 1997, 12(2): 205–210 (in Chinese)
15. Hickey K, Khan R H, Walsh J. Parametric estimation of ocean surface currents with HF radar. IEEE Journal of Oceanic Engineering, 1995, 20(2): 139–144